Available online at www.sciencedirect.com

SciVerse ScienceDirect

Journal of Nutritional Biochemistry 23 (2012) 1352–1366

Journal of Nutritional Biochemistry

Curcumin protects against thioacetamide-induced hepatic fibrosis by attenuating the inflammatory response and inducing apoptosis of damaged hepatocytes☆

Mu-En Wang[a,1], Yi-Chen Chen[a,1], I-Shu Chen[b], Shu-Chen Hsieh[c], Sheng-Shih Chen[b], Chih-Hsien Chiu[a,*]

[a]Department of Animal Science and Technology, National Taiwan University, Taiwan
[b]Department of Surgery, Veteran General Hospital-Kaohsiung, Taiwan
[c]Taiwan Institute of Food Science and Technology, National Taiwan University, Taiwan

Received 18 March 2011; received in revised form 8 August 2011; accepted 17 August 2011

Abstract

Inflammation and hepatic stellate cell (HSC) activation are the most crucial steps in the formation of hepatic fibrosis. Hepatocytes damaged by viral or bacterial infection, alcohol or toxic chemicals initiate an inflammatory response that activates collagen production by HSCs. Recent studies indicate curcumin has liver-protective effects due to its anti-inflammatory, antioxidant and anticancer activities; however, the mechanisms are not well understood. In this study, we show that curcumin protected against hepatic fibrosis in BALB/c mice *in vivo* by inhibiting HSC activation, inflammatory responses and inducing apoptosis of damaged hepatocytes. Using the thioacetamide (TAA)-induced hepatic fibrosis animal model, we found that curcumin treatment up-regulated P53 protein expression and *Bax* messenger RNA (mRNA) expression and down-regulated *Bcl-2* mRNA expression. Together, these responses increased hepatocyte sensitivity to TAA-induced cytotoxicity and forced the damaged cells to undergo apoptosis. Enhancing the tendency of damaged hepatocytes to undergo apoptosis may be the protective mechanism whereby curcumin suppresses inflammatory responses and hepatic fibrogenesis. These results provide a novel insight into the cause of hepatic fibrosis and the cytoprotective effects curcumin has on hepatic fibrosis suppression.

Keywords: Apoptosis; Curcumin; Hepatic fibrosis; Hepatocytes; Inflammation; Thioacetamide

1. Introduction

Hepatic fibrosis is caused by chronic liver injury, a continuous inflammatory response and activation of hepatic stellate cells (HSCs), which cause the accumulation of extracellular matrix (ECM) proteins, especially collagen, in liver tissue [1]. In animal wound-healing models, successful tissue repair depends on precise cell–ECM and cell–cell interactions that induce a sequential progression critical for proper tissue repair [2]. However, chronic liver injury disrupts cell–ECM and cell–cell interactions, arresting the healing process in a continuous inflammatory phase leading to the development of liver fibrosis.

Haloalkanes such as chloroform, iodoform and carbon tetrachloride have been widely used as chemical inducers of hepatic fibrosis [3]. Similar to carbon tetrachloride, thioacetamide (TAA) also induces hepatic fibrosis, and the cytotoxicity of both compounds is due to their metabolites, not the compound itself. It has been demonstrated that CYP2E1 is required for the bioactivation of TAA and TAA-induced hepatotoxicity in both rat and mouse models [4,5]. In hepatocytes, TAA is metabolized by the enzyme CYP2E1 into TAA sulfoxide and TAA-*S*,*S*-dioxide, which covalently bind other intracellular molecules and cause oxidative stress [4,6]. Cell death triggered by increased oxidative stress induces an inflammatory response, activation of HSCs, and if this is left unregulated, eventually causes hepatic fibrosis [7]. Use of TAA in hepatic fibrosis animal models has many advantages, including highly specific hepatotoxicity [8], similar progression of human hepatic fibrosis development and damage regions of the liver to those observed in human hepatic fibrosis induced by chronic liver injury.

Curcumin is a yellow compound extracted from the rhizome of turmeric (*Curcuma longa*). It has been used widely in traditional

Abbreviations: ALT, alanine aminotransferase; AST, aspartate aminotransferase; Bax, Bcl-2-associated X protein; Bcl-2, B-cell lymphoma protein 2; *Bcl-xL*, B-cell lymphoma-extra-large; BUN, blood urea nitrogen; caspase 3, cysteine-aspartic protease 3; COL1-α1, collagen type 1 α1; CYP2E1, cytochrome P450 2E1; DMSO, dimethyl sulfoxide; ECM, extracellular matrix; H&E staining, haematoxylin and eosin staining; HSC, hepatic stellate cell; IHC, immunohistochemical; MTT, methylthiazol tetrazolium bromide; NF-κB, nuclear factor κB; P53, protein 53; PBS, phosphate-buffered saline; PCNA, proliferating cell nuclear antigen; PI, propidium iodide; RT-PCR, reverse transcription polymerase chain reaction; SDS-PAGE, sodium dodecyl sulfate polyacrylamide gel eletrophoresis; TAA, thioacetamide; TNF-α, tumor necrosis factor α; TRAIL-R2, tumor necrosis factor-related apoptosis inducing ligand receptor 2; TUNEL, transferase-mediated deoxyuridine triphosphate nick-end labeling; α-SMA, α-smooth muscle actin.

☆ Conflicts of interest: The authors declare that there are no conflicts of interest in this article.

* Corresponding author. Tel.: +886 2 3366 4171; fax: +886 2 2733 4070.
E-mail address: chiuchihhsien@ntu.edu.tw (C.-H. Chiu).

[1] Mu-En Wang and Yi-Chen Chen contributed equally to this study as co-first authors.

0955-2863/$ - see front matter.
doi:10.1016/j.jnutbio.2011.08.004

Table 1
Primer sequences and amplification conditions for semiquantitative RT-PCR

Gene	Primer sequence	Product size (bp)	Annealing temperature (°C)	Cycle no.	GenBank accession no.
β-actin	F: 5′-TGTTACCAACTGGGACGACA-3′ R: 5′-TCTCAGCTGTGGTGGTGAAG-3′	394	57	35	NM_007393.2
TNF-α	F: 5′-CCACATCTCCCTCCAGAAAA-3′ R: 5′-AGGGTCTGGGCCATAGAACT-3′	259	58	38	NM_013693.2
COL1-α1	F: 5′-CACCCTCAAGAGCCTGAGTC-3′ R: 5′-GTTCGGGCTGATGTACCAGT-3′	253	60	33	NM_007742.3
Bcl-2	F: 5′-CTGGCATCTTCTCCTTCCAG-3′ R: 5′-CATGCTGGGGCCATATAGTT-3′	473	58	38	NM_009741.3
Bcl-xL	F: 5′-AGCCATTGAGTGAGGTGCTT-3′ R: 5′-AGCTCTGGGGCACCTATCTT-3′	319	58	30	NM_009743
Bax	F: 5′-CCTTTTTGCTACAGGGTTTCAT-3′ R: 5′-CAAAGTAGAAGAGGGCAACCAC-3′	279	58	31	NM_007527.3
Caspase 3	F: 5′-AGAAAAGTGACCATGGAGAACAA-3′ R: 5′-CTTCATCACCATGGCTTAGAATC-3′	385	58	42	NM_009810.2
TRAIL-R2	F: 5′-TGTGCATTCGTCTCTCTTGG-3′ R: 5′-GATGGTTGATGGAGGCACTT-3′	329	58	36	NM_020275

Table 2
Effects of chronic (8-week) administration of TAA and curcumin on the liver-to-body weight ratio, serum ALT, AST, BUN and glucose levels

Treatment	Liver/body weight ratio (%)	ALT (IU/dl)	AST (IU/dl)	BUN (mg/dl)	Glucose (mg/dl)
Control	5.10 ± 0.19^{b}	32.33 ± 5.69^{b}	72.00 ± 17.35^{b}	27.00 ± 2.65^{a}	64.33 ± 4.51^{a}
Curcumin	6.13 ± 0.73^{ab}	35.33 ± 3.21^{b}	62.67 ± 10.21^{b}	32.00 ± 4.36^{a}	95.67 ± 15.04^{a}
TAA	6.76 ± 0.32^{a}	105.33 ± 17.39^{a}	140.00 ± 25.24^{a}	31.00 ± 3.61^{a}	33.33 ± 18.82^{b}
TAA+curcumin	6.89 ± 0.56^{a}	95.33 ± 38.11^{a}	82.00 ± 26.06^{b}	35.33 ± 4.73^{a}	85.00 ± 3.00^{a}

Values are means±S.D. (n=3). Different letters above the values within each test parameter indicate significant differences between groups (P<.05).

Chinese medicine and found to have antioxidant, liver cytoprotective and cancer cytotoxic properties, but the mechanisms of these functions are not well characterized. Several reports indicate curcumin itself can act as a free radical scavenger, increase the glutathione/glutathione disulfide ratio to reduce oxidative stress and inhibit the activation and nuclear translocation of NF-κB [9,10]. In addition, a recent study postulated that curcumin protects against liver fibrosis by inactivating HSCs through activation of peroxisome

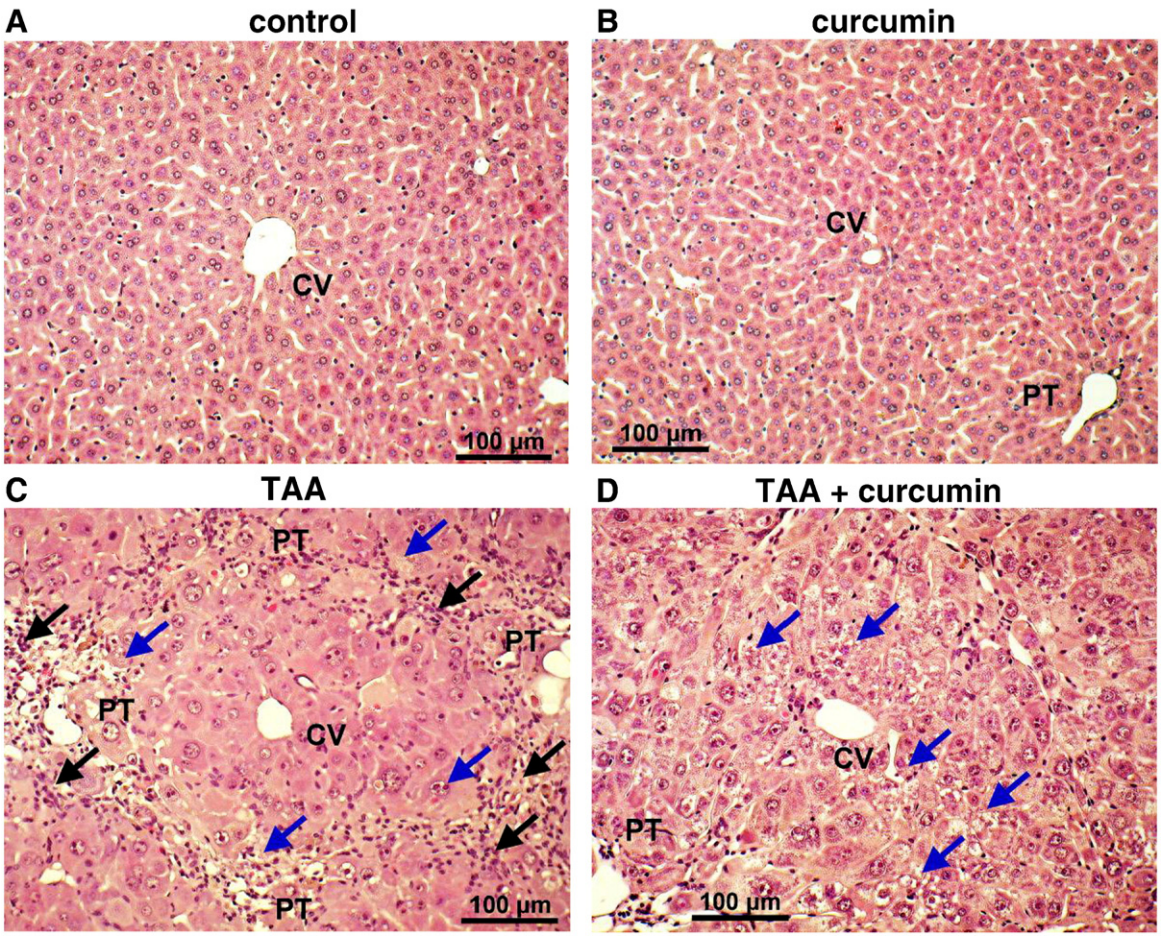

Fig. 1. Haematoxylin and eosin-stained liver sections. Liver tissues were obtained from (A) untreated control mice, (B) curcumin-treated mice, (C) TAA-treated mice and (D) TAA +Cur-cotreated mice. CV and PT refer to the central vein and portal tract, respectively. Macrophage infiltration (black arrows) was observed in livers of TAA-treated animals but was decreased in the TAA+Cur-cotreated animals. Structural abnormalities of hepatocytes caused by apoptosis or necrosis were observed in both TAA-treated and TAA+Cur-cotreated sections (blue arrows).

proliferator-activated receptor γ, which interrupts platelet-derived growth factor and epidermal growth factor signaling in activated HSCs [11].

In many studies of anti-hepatic fibrosis drugs and therapies, HSC activation was the primary target investigated due to the role of these cells in collagen production and hepatic fibrosis progression. However, we found that curcumin promoted apoptosis of damaged hepatocytes, which represents a possible alternative mechanism for the attenuation of hepatic fibrosis. Further study into the effects of curcumin on the prevention of hepatic fibrosis may provide insight into the development of more effective therapies.

2. Materials and methods

2.1. Chemicals

Curcumin and TAA were purchased from Sigma-Aldrich (St. Louis, MO). Curcumin was dissolved in sterile H_2O and dimethyl sulfoxide (DMSO) for *in vivo* and *in vitro* studies, respectively. The final concentration of DMSO was below 0.5% in culture medium for all experiments. As a chemical inducer of hepatic fibrosis, TAA [4] was dissolved in sterile phosphate-buffered saline (PBS) and culture medium for *in vivo* and *in vitro* studies, respectively.

2.2. Cell line and cell culture

AML12 cells were obtained from the Bioresource Collection and Research Center of Food Industry Research and Development Institute, Taiwan (BCRC 60326). AML12 is a nontumorigenic hepatocyte cell line derived from male CD-1 mice that overexpresses human transforming growth factor α [12]. AML12 cells were cultured in Dulbecco's modified Eagle medium/Ham's F-12 medium (Gibco, Grand Island, NY, SA) with 10% fetal bovine serum (Gibco), ITS (a 100× supplement mixture of insulin, transferrin, and selenium; Gibco), 0.1 μM dexamethasone and 1% penicillin/streptomycin (Gibco) at 37°C with 5% CO_2. Culture medium was replaced every 2–3 days. Cells were subcultured, allowed to adhere for 24 h and were at passage 5 or less for all experiments.

2.3. Animal studies

A total of 24 male BALB/c mice (6–8 weeks old) were used in this study and obtained from the Laboratory Animal Center of National Taiwan University, College of Medicine. Animals were maintained at 25°C±2°C and approximately 50%–60% relative humidity and had a 12-h light–dark cycle. A standard diet and water were freely accessible for animals.

Mice were randomly divided into four groups: control, curcumin-treated (Cur, 300 mg/kg body weight given orally), TAA-treated (TAA, 100 mg/kg body weight by intrperitoneal injection) and curcumin and TAA-cotreated (TAA+Cur). TAA and curcumin treatments were both given three times per week for an 8-week period to cause chronic liver fibrosis and evaluate the protective effects of curcumin. At the end of the treatment period, animals were sacrificed, and blood and tissue samples were harvested for downstream analyses.

2.4. Serum biochemical value analysis

Blood samples were collected from the orbital sinus and incubated for 1 h at room temperature to allow clotting. Then the serum were collected by a centrifugation at 5000*g* for 5 min and stored at −20°C until use. Serum alanine aminotransferase (ALT), aspartate aminotransferase (AST), blood urea nitrogen (BUN) and glucose levels were assayed using an ARKRAY SPOTCHEM SP-4410 automatic dry chemistry analyzer.

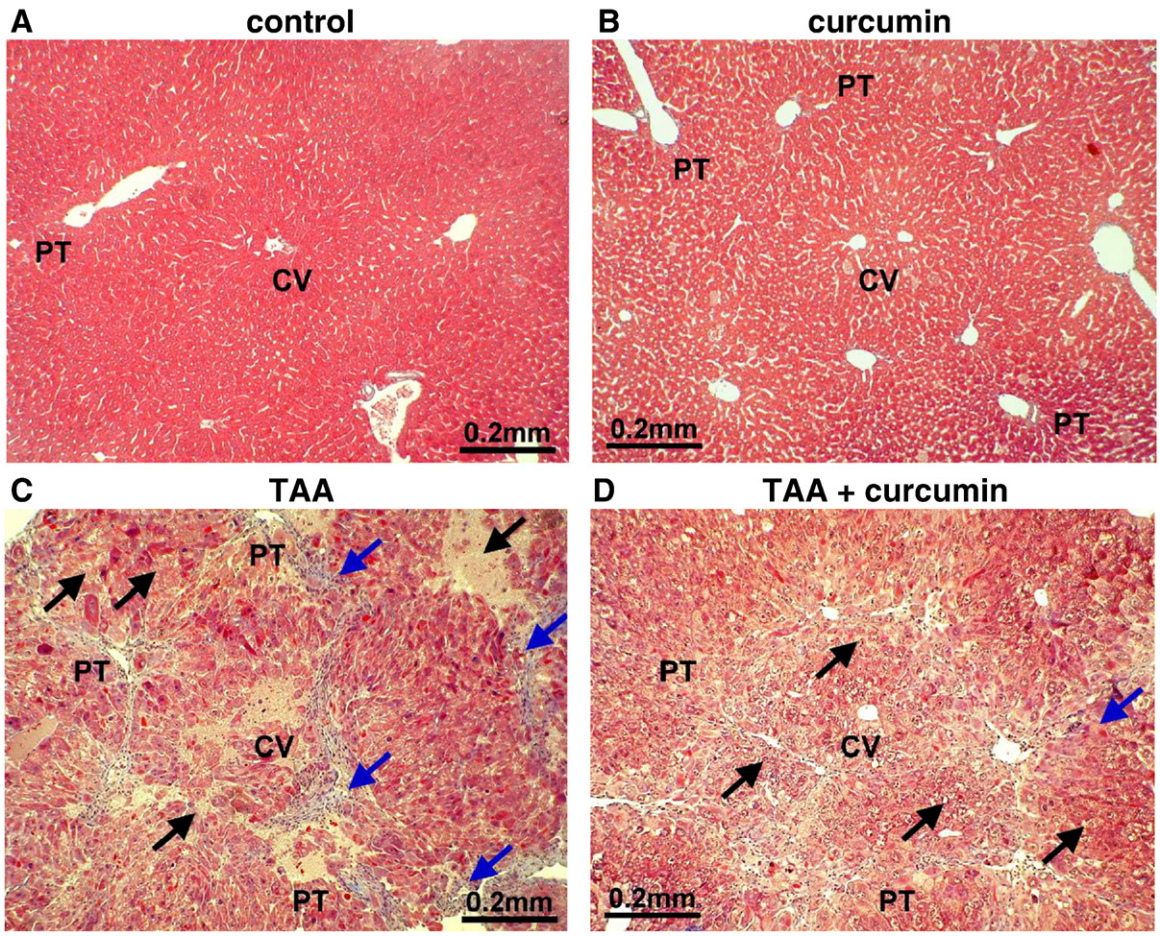

Fig. 2. Liver sections with Masson's trichrome staining. Liver tissues were obtained from (A) untreated control mice, (B) curcumin-treated mice, (C) TAA-treated mice and (D) TAA +Cur-cotreated mice. CV and PT refer to the central vein and portal tract, respectively. Hepatic fibrosis (stained in blue, blue arrows) was observed in TAA-treated liver sections but was reduced in TAA+Cur-cotreated liver sections. Vacuoles caused by cell necrosis or apoptosis are indicated (black arrows).

2.5. Semiquantitative reverse transcriptase polymerase chain reaction gene expression analysis

Total RNA was isolated from liver tissues (stored at −80°C) using TRIzol reagent (Invitrogen, Carlsbad, CA) and purified using the RNeasy Mini kit (QIAGEN, Valencia, CA), following the manufacturer's instructions. Complementary DNA (cDNA) was synthesized using the ThermoScript RT-PCR kit for First-Strand cDNA Synthesis (Invitrogen) with an oligo $(dT)_{20}$ primer. Semiquantitative reverse transcriptase polymerase chain reactions (sqRT-PCR) for cDNA samples were performed using SuperHot Taq DNA polymerase (BIORON, Ludwigshafen am Rhein, Germany) with specifically designed primers on a MyCycler Thermal Cycler (Bio-Rad, Hercules, CA). sqRT-PCR products were then separated by agarose gel (2%) electrophoresis and visualized by ethidium bromide staining on a UVP BioDoc-It imaging system. Pixel intensity of bands was quantified using UVP VisionWorksLS Analysis software. In each treatment group, three independent liver samples from different animals were used. All values were normalized to sqRT-PCR product levels of β-actin as an internal control. Primer sequences and sqRT-PCR conditions used in this study are listed in Table 1.

2.6. Histological sections and immunohistochemical staining

Liver tissues from mice were fixed in 10% formalin in sterile PBS, embedded in paraffin and sectioned. For analysis of overall liver morphology and hepatic collagen accumulation, haematoxylin and eosin staining (H&E), Masson's trichrome and Sirius red staining (Sigma-Aldrich) were performed. For semiquantitative collagen accumulation assays, percentage of stained collagen fibers area in random fields was quantified using ImageJ software version 1.45h. For immunohistochemical (IHC) analysis, VECTASTAIN elite ABC kit (Vector Laboratories, Burlingame, CA) was used with specific antibodies for proliferating cell nuclear antigen (PCNA, MS-106; Thermo Scientific, Fremont, CA), active caspase 3 (cysteine-aspartic protease 3, ab13847; Abcam, Cambridge, UK) and α-smooth muscle actin (α-SMA, ab5694; Abcam).

2.7. Methylthiazol tetrazolium cell viability assay

To determine the proper dose of curcumin and TAA for the *in vitro* studies, we examined the cytotoxicity of these compounds using the methylthiazol tetrazolium (MTT) cell viability assay [13]. AML12 cells were cultured in 96-well plates at a density of 1×10^5 cells/ml, 200 μl of cell suspension per well for 24 h prior to curcumin and TAA treatment. Cells were then treated with media containing increasing concentrations of curcumin (0, 5, 10, 20, 40 and 80 μM) or TAA (0, 25, 50, 100, 200 and 400 mM) for 24 and 48 h. After treatment, the cells were incubated with 50 μl MTT solution (5 mg/ml, dissolved in PBS) and 150 μl medium for 4 h. Conversion of MTT to formazan was determined by dissolving formazan in 200 μl DMSO with 25 μl Sorensen's buffer (0.1 M glycine+0.1 M NaCl, pH=10.5) in the dark and determining the absorbance at 570 nm in a μQuant microplate spectrophotometer (BioTek Instrument, Winooski, VT).

2.8. Transferase-mediated deoxyuridine triphosphate nick-end labeling cell apoptosis assay

We performed the terminal deoxynucleotidyl transferase-mediated deoxyuridine triphosphate nick-end labeling (TUNEL) assay on liver section and AML12 cell using the *In Situ* Cell Death Detection Kit (Roche Applied Science, Indianapolis, IN) following the manufacturer's instructions. Cells for this assay were cultured on Lab-Tek II Chamber slides (two chambers per slide, Nunc) at a density of 1×10^5 cells/ml, 1 ml suspension per chamber. Cells treated with staurosporine (Sigma-Aldrich), a nonselective protein kinase inhibitor [14] were used as positive control.

2.9. Annexin V–FITC cell apoptosis assay

AML12 cells were used to perform an annexin V–FITC apoptosis assay using the annexin V–FITC Apoptosis Detection Kit (Strong Biotech, Nankang, Taiwan), which combine annexin V and propidium iodide (PI) staining for the detection of altered membrane phosphatidylserine distribution and cell membrane integrity [15]. Cells were cultured as for the TUNEL assay and the staining was performed according to the manufacturer's instructions.

2.10. Western blot analysis of P53 protein

For Western blot analysis of P53 protein, liver tissues were homogenized, lysed using a Vibra-Cell ultrasonic processor (Sonics, Newtown, CT) and dissolved in the Complete Protease Inhibitor Cocktail (Merck, Darmstadt, Germany) solution. Extracted protein was assayed using the Bradford protein assay (Bio-Rad). Samples (20 μg/lane) were separated by SDS-PAGE on a 12% resolving gel and then transferred to polyvinylidene fluoride membranes. Detection of P53 and glyceraldehyde 3-phosphate dehydrogenase, as the internal control, was performed with specific primary antibodies from Abcam (ab26) and Novus (NB300-327) and subsequently detected by horseradish peroxidase-conjugated secondary antibodies (Jackson Immuno-Research). Protein bands were visualized with Novex ECL Chemiluminescent Reagent (Invitrogen).

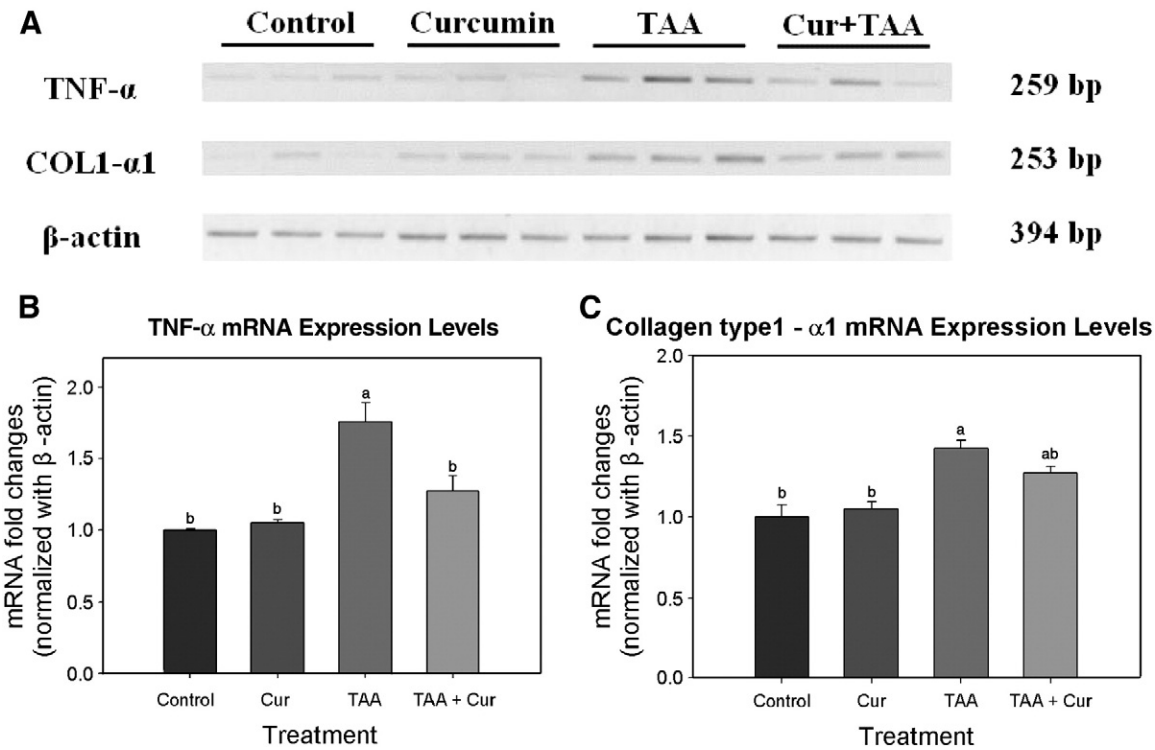

Fig. 3. Effects of curcumin on inflammation and fibrosis-related gene expressions. (A) mRNA expression fold changes of TNF-α and COL1-α1 were assayed by sqRT-PCR and analyzed by agarose gel electrophoresis. Levels of TNF-α (B) and COL1-α1 (C) were quantified using the UVP VisionWorksLS Analysis Software. Values of each bar are means±S.E. (n=3). In each treatment group, three independent liver samples from different animals were used. β-Actin was used as an internal control for calculating mRNA fold changes. a–b, Columns with different letters differ significantly (P<.05).

2.11. Statistical analysis

The experiment was conducted using a 2×2 factorial arrangement of treatment design. The interaction effect (TAA×Curcumin) and main effect (TAA and curcumin) were analyzed. All significant differences in the interaction effect and main effect were tested using an ANOVA test at .05 probability level. When a significant difference in the interaction effect was determined, the Holm–Sidak test at .05 probability level was used to test differences between combination treatments. All statistical analyses of data were performed using SigmaStat version 3.5.

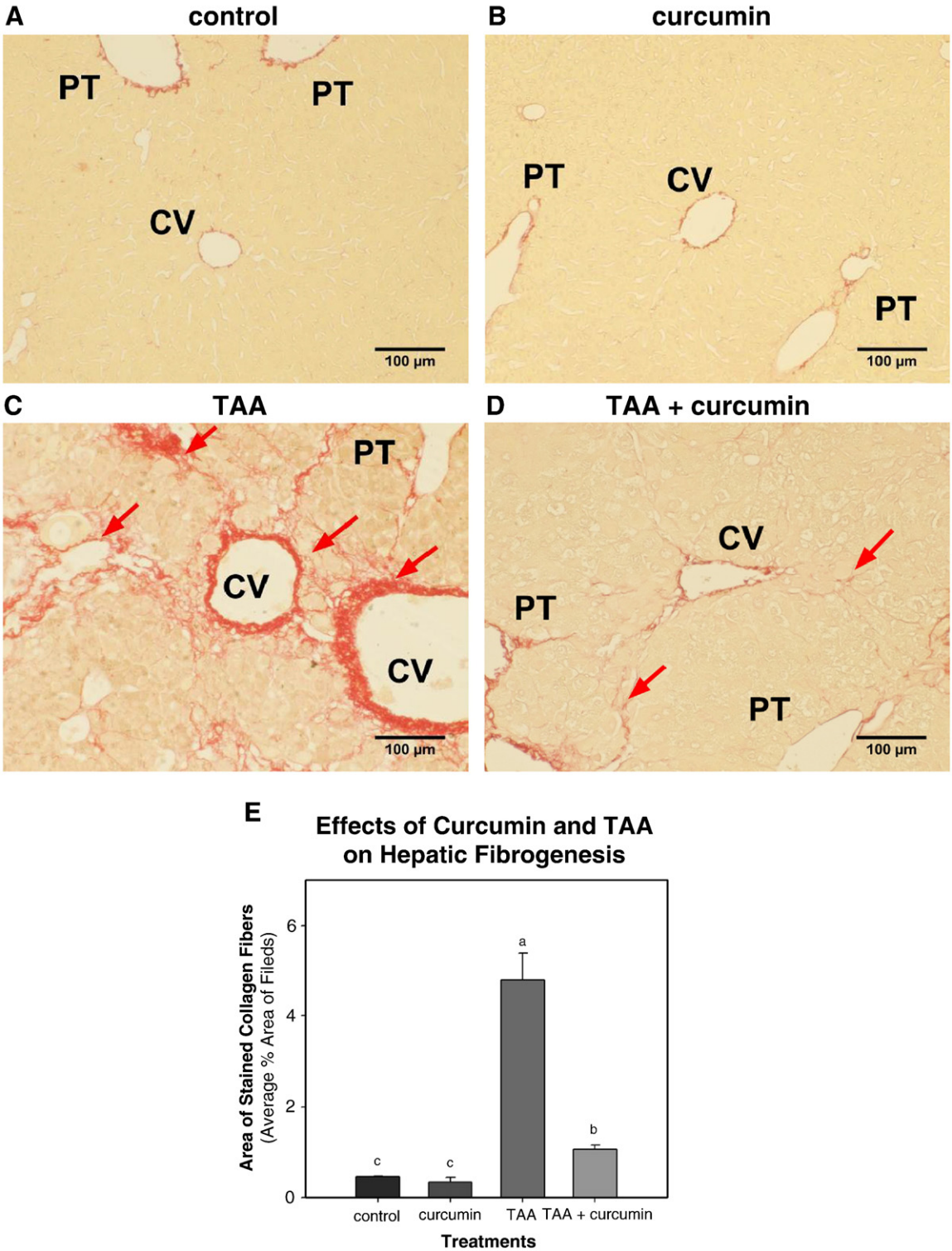

Fig. 4. Sirius red staining and semiquantitative collagen accumulation assays. Liver sections obtained from (A) untreated control mice, (B) curcumin-treated mice, (C) TAA-treated mice and (D) TAA+Cur-cotreated mice were stained with Sirius red. Area ratio of stained collagen was quantified by ImageJ software (version 1.45h) and shown in (E). Values of each bar are means±S.D. (n=4). a–c, Columns with different letters differ significantly (P<.05).

3. Results

3.1. TAA treatment had multiple effects on the liver

To establish the feasibility of the mouse model of TAA-induced hepatic fibrosis and possible effects of curcumin on hepatic fibrogenesis, we first assayed the liver-to-body weight ratio; serum ALT, AST and BUN levels; and serum glucose levels of 6- to 8-week-old male BALB/c mice from untreated control mice, TAA-treated (100 mg/kg body weight for 8 weeks), curcumin-treated (300 mg/kg body weight) mice and TAA cotreated with curcumin mice. TAA treatment elevated ($P<.05$) the liver-to-body weight ratio, increased serum ALT and AST levels and decreased serum glucose levels (Table 2). However, no significant differences in serum BUN levels were found between the treatment and control groups. The increased liver-to-body weight ratio was likely due to swelling of the liver from a chronic inflammatory response. In addition, elevated serum ALT and AST levels indicate the release of these cytosolic enzymes from hepatocytes due to cell lysis. Finally, reduced serum glucose levels indicate the observed liver damage resulted in liver dysfunction.

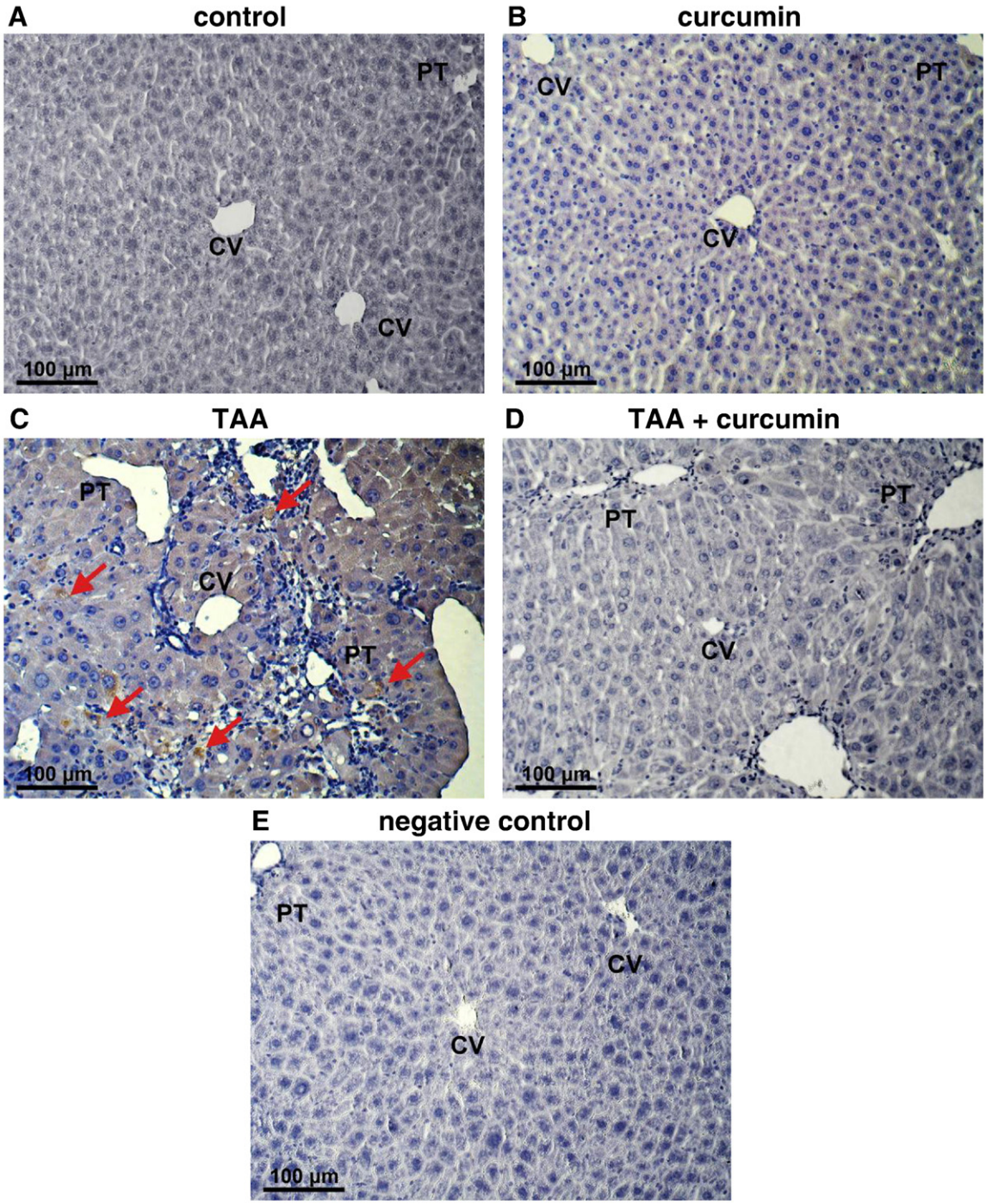

Fig. 5. Immunohistochemical staining for activated HSC in liver sections. Liver tissues were obtained from (A) untreated control mice, (B) curcumin-treated mice, (C) TAA-treated mice and (D) TAA+Cur-cotreated mice. Negative-control sections (E) were stained without adding the primary antibody. α-SMA, a marker of activated HSCs, is stained in brown (red arrows). Activated HSCs were observed in TAA-treated liver sections, but no activated HSCs were found in TAA+Cur-cotreated liver sections.

Therefore, the 8-week TAA treatment induced liver damage and dysfunction without affecting other organs, such as the kidneys, because serum BUN levels remained unchanged. Although the serum ALT was not significantly reduced by curcumin cotreatment, reduction of serum AST might reflect the possible protective effect of curcumin on hepatocytes since the mitochondrial AST is released only when the cells are severely disintegrated [16].

3.2. Curcumin and TAA caused morphological change in liver tissues

Next, we used the mouse model of TAA-induced liver damage to determine if the cytoprotective properties of curcumin could reduce or prevent liver damage. After the 8-week treatment, liver tissues were collected, embedded in paraffin and sections were made. Histological examination of H&E- and Masson's trichrome-stained

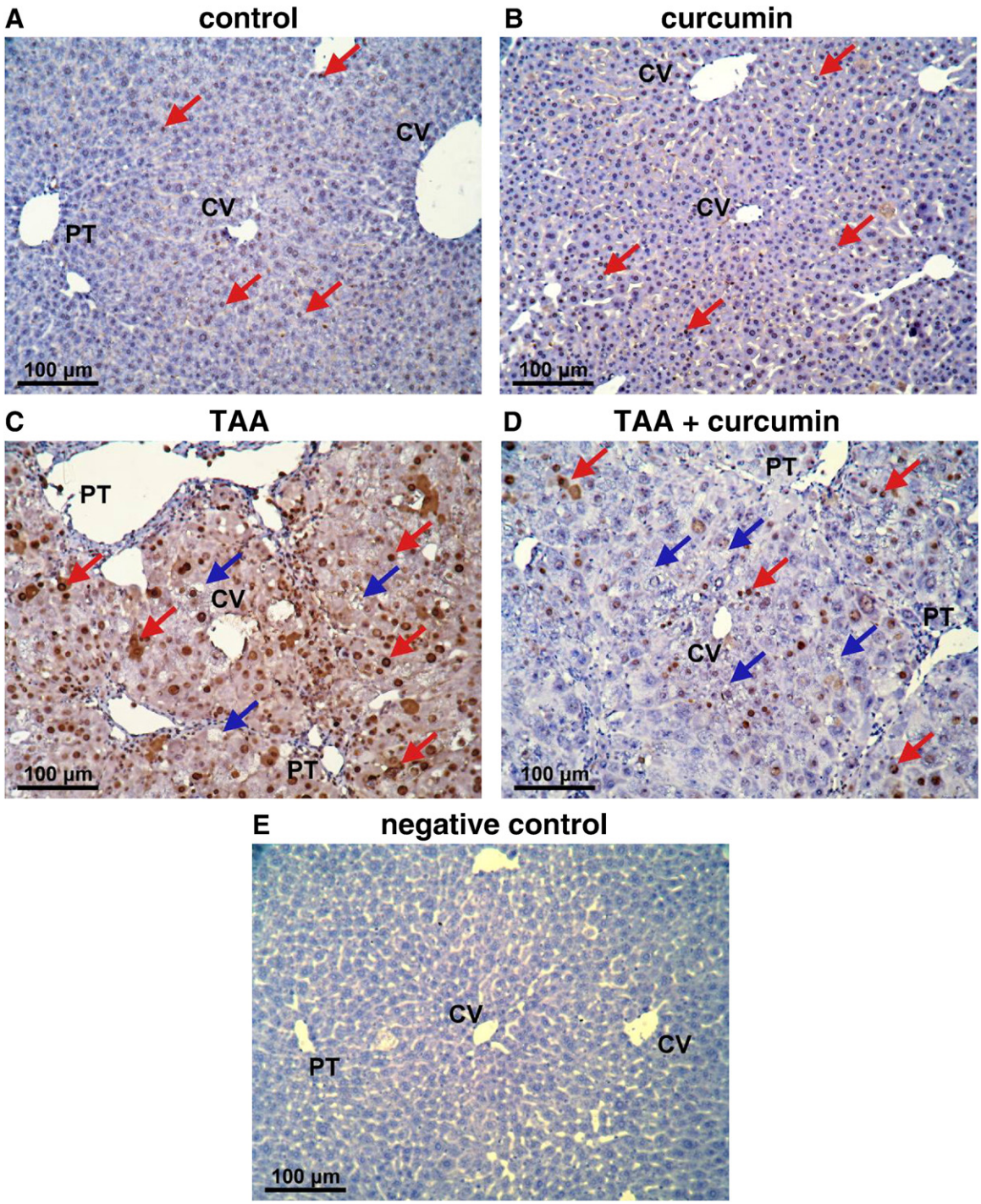

Fig. 6. Immunohistochemical staining for proliferating cells in liver sections. Liver tissues were obtained from (A) untreated control mice, (B) curcumin-treated mice, (C) TAA-treated mice and (D) TAA+Cur-cotreated mice. Negative control sections (E) were stained without adding the primary antibody. Proliferating cell nuclear antigen, a marker of proliferating cells, is stained in brown (red arrows). Vacuoles caused by cell necrosis or apoptosis are indicated by blue arrows. The number of proliferating cells was lower in the TAA+Cur-cotreated group then the TAA treated group.

sections was performed to determine the extent of liver injury and fibrosis for each section.

Haematoxylin and eosin-stained liver sections (Fig. 1) of the TAA-only treated animals showed a macrophage accumulation (Fig. 1C, black arrows) that was absent in the untreated control and curcumin-treated animals (Fig. 1A and B). The macrophage accumulation was present but substantially reduced in the TAA+Cur-cotreated animals (Fig. 1D). This indicated curcumin cotreatment inhibited TAA-induced liver inflammation. Interestingly, we also found more pronounced structural abnormalities of the hepatocytes such as unclear stained cytoplasm, disruptive cells without clear cell boundaries and apoptotic-body-like vacuoles in the TAA+Cur-cotreatment group than in the TAA-treated animals (Fig. 1C and D, blue arrows). Theses abnormalities were likely due to hepatocytes undergoing necrosis or apoptosis.

3.3. Effects of curcumin and TAA on liver fibrogenesis

Masson's trichrome staining of liver sections was used to determine the extent of hepatic fibrosis induced by TAA treatment in the presence and absence of curcumin (Fig. 2). No fibrosis was detected in the liver sections of the untreated control or curcumin-treated animals (Fig. 2A and B). In contrast, extensive fibrosis was observed in the liver sections from TAA-treated animals (Fig. 2C). Sections from the TAA+Cur-cotreated animals (Fig. 2D) showed greater fibrosis than the untreated or curcumin-only-treated animals, but the degree of fibrosis was substantially less than the TAA-alone-treated animals. Thus, TAA treatment for 8-week induced hepatic fibrosis (indicated by blue arrows), but cotreatment with curcumin reduced collagen accumulation in the liver. As observed in the H&E-stained sections, the hepatocytes of the TAA+Cur-cotreated animals had more vacuolation due to apoptosis or necrosis than the TAA-treated group.

3.4. Curcumin attenuated inflammatory responses by down-regulating tumor necrosis factor α gene expression

Since curcumin treatment reduced the infiltration of macrophages and accumulation of collagen in TAA-induced liver injury, we performed sqRT-PCR for analysis of tumor necrosis factor α (TNF-α) and collagen type I α 1 (COL1-α1) messenger RNA (mRNA) levels (Fig. 3). Tumor necrosis factor α is a proinflammatory cytokine and Col1-α1 is the most abundant type of collagen found in scar tissue. Products from the sqRT-PCR were analyzed by agarose gel electrophoresis (Fig. 3A) and quantitated to determine the relative levels (Fig. 3B and C). The mRNA levels of both TNF-α (Fig. 3B) and Col1-α1 (Fig. 3C) were increased ($P<.05$) in the livers of TAA-treated mice. Only the TNF-α, but not Col1-α1 mRNA was significantly decreased in the livers of TAA+Cur-cotreated animals. Curcumin cotreatment reduced the TNF-α to levels similar to the untreated control and curcumin-treated groups, indicating that curcumin can block the TAA-induced inflammatory response *in vivo* by inhibition of TNF-α expression.

3.5. Curcumin reduced TAA caused collagen accumulation in vivo

To confirm the antifibrotic effects of curcumin, we performed Sirius red staining with semiquantitative assays using ImageJ software (version 1.45h). In the untreated control and curcumin-treated mice, collagen fibers (stained in red) were only detected around the central vein and portal triad (Fig. 4A and B). Consistent with the results shown in Masson's trichrome staining, the increased collagen accumulation induced by TAA treatment was reduced in TAA+Cur-cotreated group (Fig. 4C and D). Although the Col1-α1 mRNA level was not significantly reduced by curcumin cotreatment, quantitative results show significant reduction of collagen accumulation in the livers of cotreated animals (Fig. 4E).

3.6. Curcumin blocked HSC activation

We next sought to determine the mechanisms by which curcumin exerts its anti-inflammatory and antifibrotic properties. We first determined the degree of HSC activation in liver tissues using IHC staining for α-SMA (Fig. 5), a marker of activated HSCs. No α-SMA was observed in the untreated control or curcumin-treated groups (Fig. 5A and B). Substantial α-SMA was observed in the livers of TAA-treated animals (Fig. 5C), but, as in the negative control, no α-SMA was detected in the livers of the TAA+Cur-cotreated animals (Fig. 5D).

3.7. Curcumin inhibited the proliferation of damaged hepatocytes

The next step was to investigate the cause of pronounced vacuolation of hepatocytes in the TAA- and curcumin-treated mice. First, to determine the degree of cellular proliferation, IHC staining for PCNA, a proliferation marker for different cell types including hepatocyte was used [17] (Fig. 6). Proliferating cell nuclear antigen was expressed at a low basal level in hepatocytes of untreated control and curcumin-treated mice (Fig. 6A and B). In contrast, PCNA expression was up-regulated in hepatocytes of the TAA-treated animals, indicating increased proliferation to repair the damaged liver tissue (Fig. 6C). Coadministration of curcumin with TAA substantially lowered the expression of PCNA in the hepatocytes, indicating curcumin inhibits the proliferation of damaged hepatocytes (Fig. 6D).

3.8. Curcumin increased the expression of P53

Since curcumin only inhibited cell proliferation in the TAA+Cur cotreatment group, we hypothesized that this effect was related to cell cycle checkpoints involved in DNA repair. The tumor suppressor P53 is a crucial protein that participates in DNA damage repair, cell cycle regulation and many other cellular pathways. It is normally expressed at a low level, and protein levels are regulated through a ubiquitin-mediated degradation pathway [18]. Upon DNA damage, the P53-mediated DNA response pathway is activated, arresting the cell cycle to prevent cell proliferation until all the DNA damage is repaired [19]. Using Western blot analysis of liver homogenates, we found expression of P53 was up-regulated in both the curcumin-treated and TAA+Cur-cotreated mice livers (Fig. 7). A slight increase in P53 expression was also found in only TAA-treated mice. These data suggest that curcumin inhibits proliferation of damaged cells through up-regulation of P53 expression, which arrests the cell cycle at a DNA damage checkpoint.

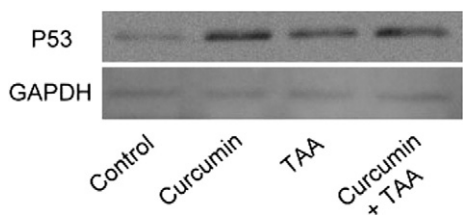

Fig. 7. Curcumin-increased expression of P53 protein. Western blot analysis of liver homogenates for P53. Detection of glyceraldehyde 3-phosphate dehydrogenase was performed as an internal control.

3.9. Curcumin cotreatment increased cell apoptosis in vivo

As a tumor suppressor, P53 not only can induce cell cycle arrest and DNA repair through its regulations on a wide variety of genes but also promotes apoptosis when unrepairable DNA damage occurs [20]. Thus, we hypothesized that curcumin might also attenuate hepatic fibrosis by promoting damaged hepatocytes to undergo apoptosis. To verify this hypothesis, we performed TUNEL assays and IHC staining for active caspase 3 on liver sections obtained from different treating groups. Cleavage and activation of caspase 3 is the final decision for cell to execute apoptosis; therefore, the presence of active caspase 3 could be considered as a marker of the early-stage apoptosis [21,22]. As shown in Fig. 8, positively labeled cells were similarly increased in both TAA+Cur-cotreated groups (Fig. 8C and D) compared to untreated control and curcumin-treated groups (Fig. 8A and B). However, in the results of TUNEL assay, the TUNEL positively labeled cells (late apoptotic or necrotic cells) were significantly increased under curcumin cotreatment (Fig. 9G). Also, with the Hoechst 33342

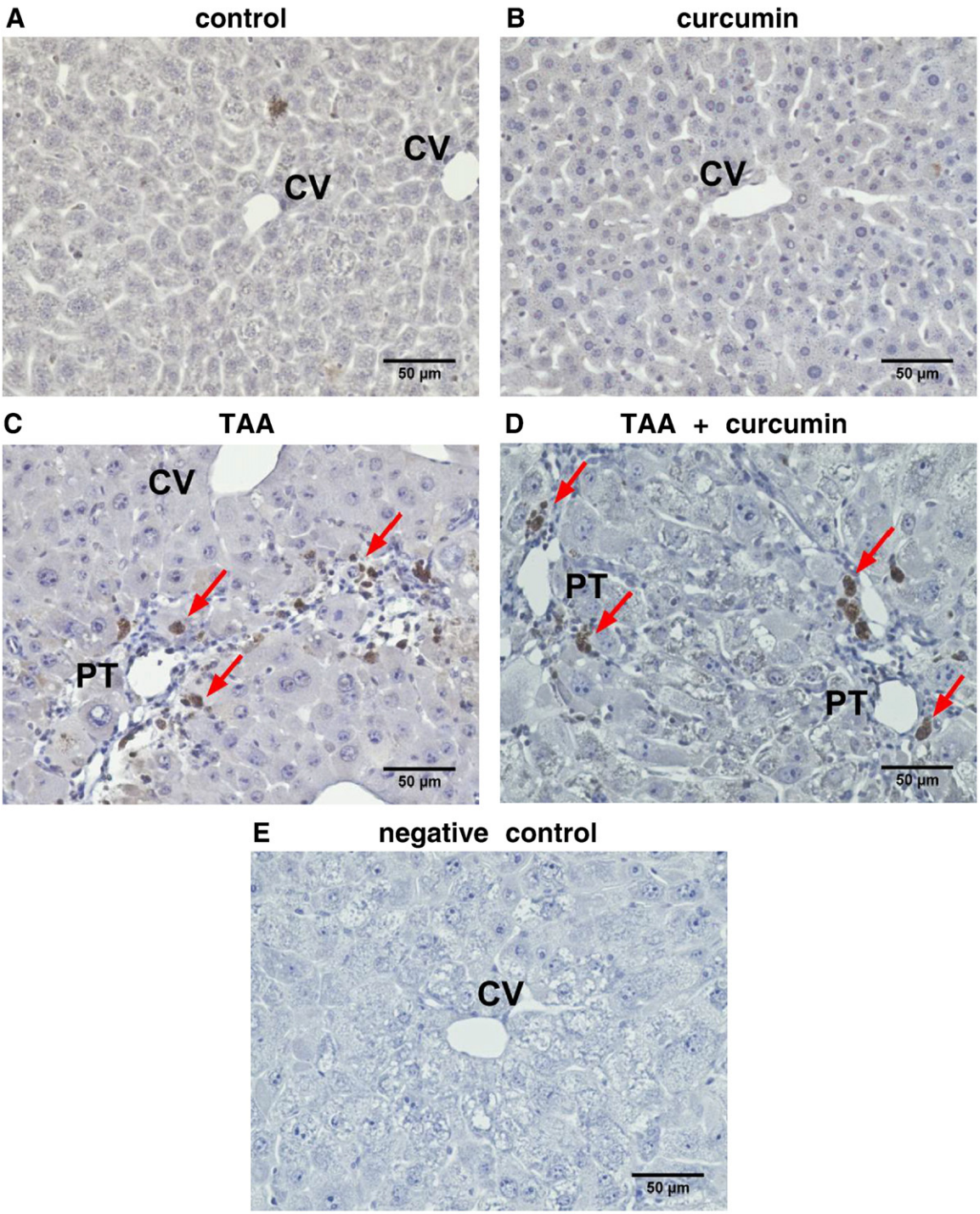

Fig. 8. Immunohistochemical staining for active caspase 3 in liver sections. Liver tissues were obtained from (A) untreated control mice, (B) curcumin-treated mice, (C) TAA-treated mice and (D) TAA+Cur-cotreated mice. Negative control sections (E) were stained without adding the primary antibody. The positively stained cells were indicated by red arrows. Positively stained cells were similarly increased in TAA-treated and TAA+Cur-cotreated groups, compared to control and curcumin groups.

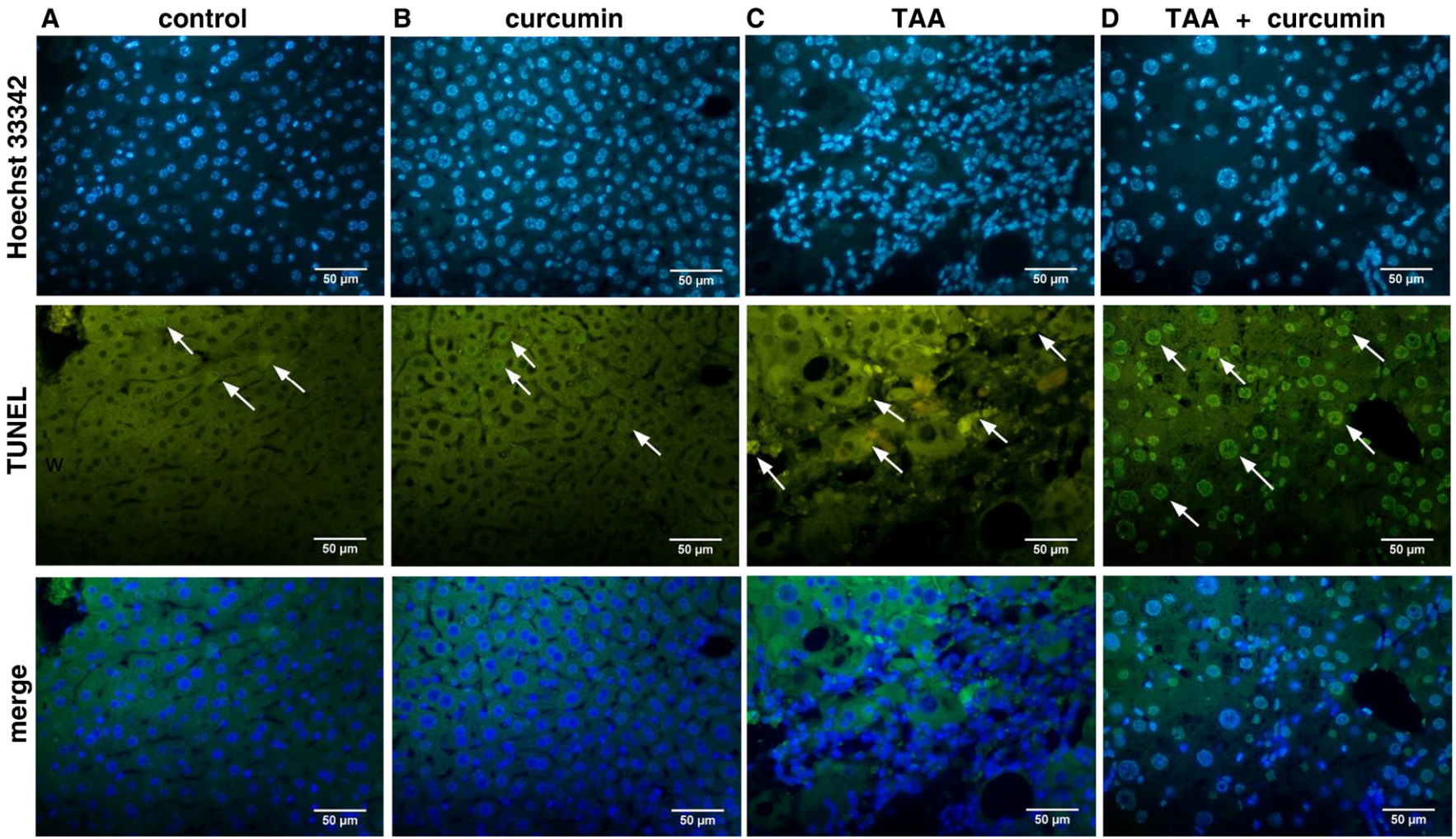

Fig. 9. TUNEL apoptosis assays on liver sections obtained from (A) untreated control mice, (B) curcumin-treated mice, (C) TAA-treated mice and (D) TAA+Cur-cotreated mice. Hoechst 33342 was used for nuclear counterstain. (E) DNase I-treated and (F) non-TdT-treated sections were used as positive and negative controls, respectively. (G) Shows the ratios of TUNEL-positive cell counts in these four treatment groups. Values of each bar are means±S.D. (n=4). a–c, Columns with different letters differ significantly (P<.05).

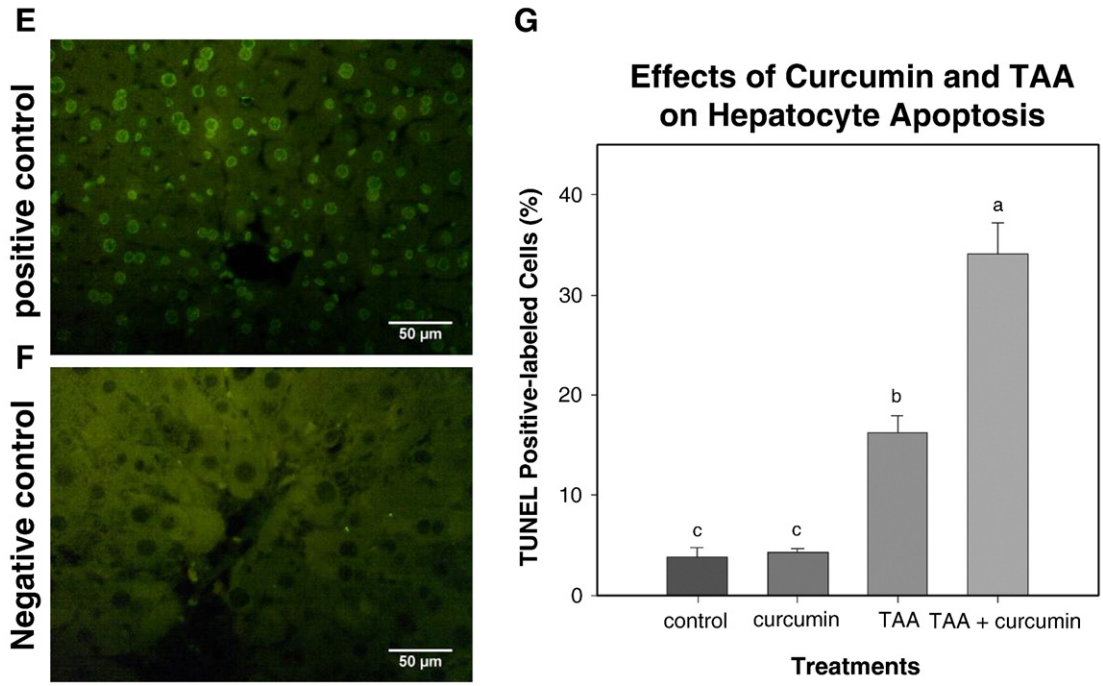

Fig. 9 (*continued*).

counterstain, we found that the necrotic cell death, characterized by incomplete cell structures and leak of fragmented DNA to the cytoplasm, found in TAA treated group (Fig. 9C) was shifted to apoptotic cell death under curcumin cotreatment (Fig. 9D).

3.10. Curcumin effects on apoptosis-related gene expressions

To further investigate the possible mechanisms by which curcumin shifts the necrotic cell death to apoptosis, we analyzed the mRNA expression levels of apoptosis regulating genes using sqRT-PCR. sqRT-PCR products were analyzed by agarose gel electrophoresis (Fig. 10A) and quantitated to determine their relative levels (Fig. 10B–F). Consistent with our assumption, we found that curcumin significantly reduced the expression of the antiapoptosis gene Bcl-2 (Fig. 10B), which was up-regulated by TAA treatment. Also, coadministration of curcumin with TAA slightly down-regulated the antiapoptotic *Bcl-XL* gene (Fig. 10C) and up-regulated proapoptotic gene *Bax* (Fig. 10D) expressions. However, the levels of other apoptosis-related genes, such as caspase 3 (Fig. 10E) and TRAIL-R2 (Fig. 10F), were not altered by curcumin. These data provide evidence that curcumin may promote apoptosis in TAA-damaged hepatocytes by regulating apoptosis-related gene expressions.

3.11. Curcumin triggered apoptosis of TAA-damaged hepatocytes

Since curcumin simultaneously up-regulated proapoptosis genes and down-regulated antiapoptosis genes, we next evaluated the ability of curcumin to promote apoptosis of hepatocytes using TUNEL assays and annexin V–FITC staining on AML12 cells. AML12 is a nontumorigenic hepatocyte cell line derived from male CD-1 mice that overexpresses human transforming growth factor α [12]. First, we determined a proper subcytotoxic dose of both TAA and curcumin by performing an MTT cell viability assay (Fig. 11). Based on these data, we choose 20 μM and 200 mM as the concentrations for following curcumin (Fig. 11A) and TAA (Fig. 11B) treatments, respectively.

We performed a TUNEL apoptosis assay on AML12 cells (Fig. 12). Treatments of DNase I and staurosporine, a pan-protein kinase inhibitor, were used as positive controls for DNA fragmentation and apoptosis induction, respectively (Fig. 12C and H). Results of the TUNEL assay showed that TAA treatment slightly increased the number of apoptotic cells (Fig. 12E), but when pretreated with curcumin for 12 h (Fig. 12F) or cotreated with curcumin for 24 h (Fig. 12G), apoptosis was substantially promoted. This suggests that curcumin not only prevents damaged hepatocytes from proliferating but also promotes them to undergo apoptosis.

Apoptosis is a type of programmed cell death that can be triggered by intrinsic or extrinsic signals [23]. Since many molecules participated in different apoptosis signaling pathways, we confirmed the results of the TUNEL assays, which only detect DNA fragmentation that occurs late in apoptotic cells, by staining cells with FITC-conjugated annexin V and PI (Fig. 13). These stains measure the integrity of the plasma membrane and detect the exposure of phosphatidylserine on the outer leaflet of the plasma membrane with annexin V [24]. Additionally, PI is a membrane-impermeable fluorescent DNA-intercalating dye that will only stain the nucleus of necrotic or late apoptotic cells with low membrane integrity.

TAA treatment increased cell necrosis (PI-positive but annexin V-negative) and slightly increased apoptosis (annexin V-positive but PI-negative) (Fig. 13D). However, in TAA+Cur-cotreated cells, there were fewer necrotic cells and more apoptotic cells than in the TAA treated group (Fig. 13E). Thus, curcumin shifted the cell death phenotype from necrosis to apoptosis, which *in vivo* would reduce the release of inflammatory mediators that would prevent chronic liver damage and fibrosis.

4. Discussion

Curcumin is known to reduce oxidative stress, decrease inflammatory responses [10], inhibit the activation of HSCs [5,11,25] and promote apoptosis by regulating several different pathways in different types of cancer cells, such as hepatic carcinoma [26], prostate cancer [27,28] and lung cancer [29]. To clarify the curcumin-induced hepatoprotective mechanisms that prevent liver diseases and confirm recent *in vitro* studies, we established a model

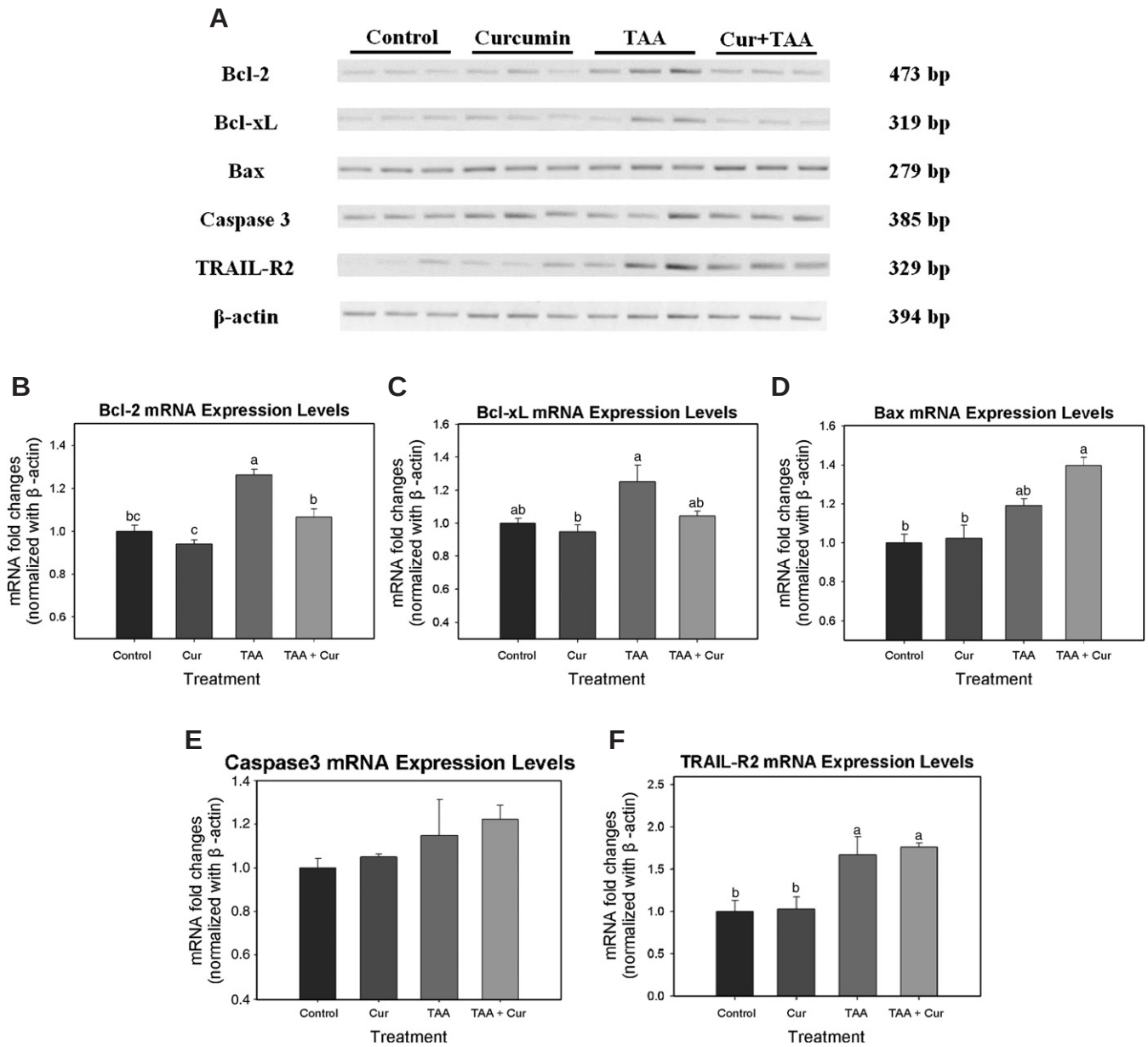

Fig. 10. Effects of curcumin on apoptosis-related gene expressions. (A) mRNA expression fold changes of Bcl-2, Bcl-xL, Bax, caspase 3 and TRAIL-R2 in liver homogenates were assayed by sqRT-PCR and analyzed by agarose gel electrophoresis. The electrophoresis results of (B) Bcl-2, (C) Bcl-xL, (D) Bax, (E) caspase 3 and (F) TRAIL-R2 were quantified using the UVP VisionWorksLS Analysis Software. Values of each bar are means±S.E. (n=3). In each treatment group, three independent liver samples from different animals were used. β-actin was used as an internal control for calculating mRNA fold changes. a–c, Columns with different letters differ significantly (P<.05).

of TAA-induced hepatic fibrosis in male BALB/c mice. Chronic (8 weeks) and low-dose (100 mg/kg body weight) TAA treatment effectively induced liver injury and dysfunction and caused hepatic fibrosis without damage to other organs. Coadministration of curcumin for TAA-treated animals substantially reduced collagen accumulation, and therefore fibrosis, between hepatic lobules. While we confirmed the reduction in α-SMA found by others [30], we also demonstrated the curcumin-induced apoptosis of damaged hepatocytes, constituting a new pathway for attenuating hepatic inflammatory responses and fibrogenesis.

We expected curcumin to inhibit hepatic fibrogenesis by suppressing hepatic inflammatory responses and HSC activation; however, we found that curcumin not only regulated HSC activation but also the cell cycle progression of hepatocytes. In the postnecrotic proliferative response [31], first, we found that curcumin significantly reduced the number of proliferating hepatocytes in TAA-injured liver using PCNA as the cell proliferation marker. Next, we showed that curcumin up-regulates P53 expression in hepatocytes and the increased P53 expression was not simply dependent on TAA-induced injury. These data suggest that the increased P53 acts as a cell cycle regulator in the TAA-damaged cells by arresting them in G1 phase when DNA damage is detected [32]. However, the decrease in cell proliferation caused by curcumin treatment cannot be explained only by up-regulation of P53, because the level of P53 expression in TAA-treated and TAA+Cur-cotreated livers was similar, unlike the levels of PCNA that were substantially different. Thus, we examined the induction of apoptosis, since in the presence of irreparable DNA damage, P53 will also initiate apoptotic cell death [33,34].

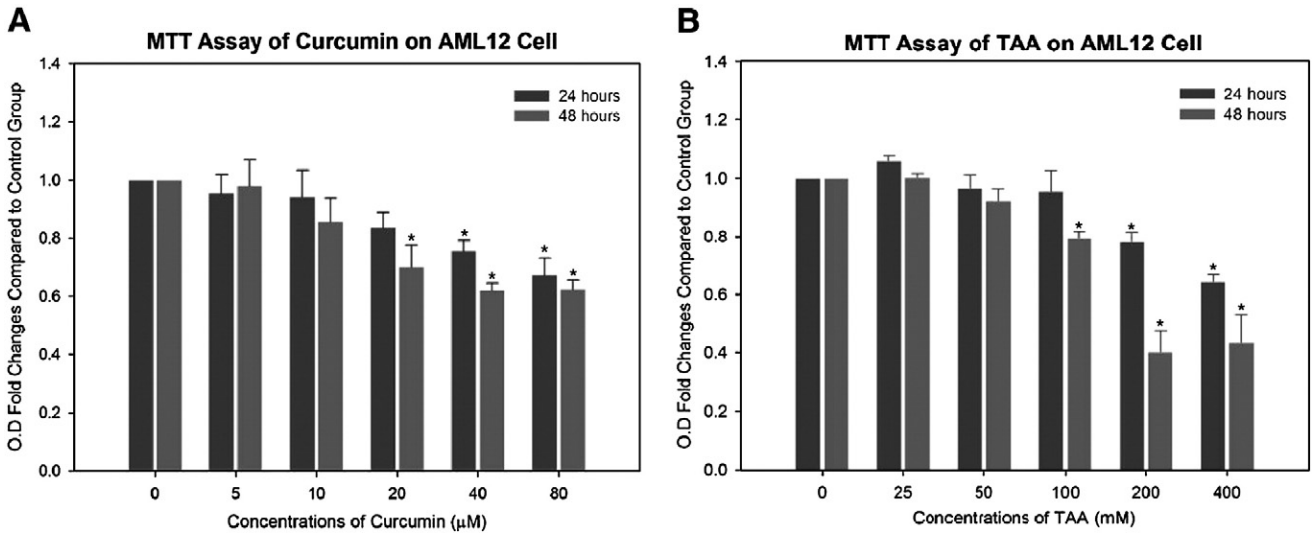

Fig. 11. Cytotoxicity of (A) curcumin and (B) TAA measured by MTT assays. AML12 cells were cultured in 96-well plates (1×10^5 cells/ml, 200 μl/well) 24 h prior to curcumin and TAA treatment for the indicated time (24 or 48 h). Then, cells were incubated with MTT-containing medium for an additional 4 h. OD values were read at 570 nm, normalized to the control group and expressed as the fold change. *Significant differences compared to the control group ($P<.05$).

When chronic liver injury occurs, intracellular components released from necrotic cells are able to activate immune cells and trigger the reactive oxygen species-mediated cell killing process, which leads to more oncotic necrosis and amplified inflammation [35]. The results of continuous inflammatory response are HSC overactivation and hepatic fibrosis. On the contrary, apoptosis is a type of programmed cell death occurring in normal physiological conditions. Unlike necrosis, properly induced apoptotic cell death does not induce inflammatory response due to the maintenance of membrane integrity. Recent studies also indicate that apoptotic cells have inhibitory effects on hepatic inflammatory responses [36].

Consistent with our conjectures, curcumin promotes TAA-damaged cells to undergo apoptosis rather than necrosis by up-regulating Bax and down-regulating Bcl-2 and Bcl-xL mRNA expression levels *in vivo*. These data allow us to postulate a new model of the hepatoprotective mechanisms induced by curcumin that is illustrated in Fig. 14. In wound healing, ECM remodeling and cell proliferation are necessary for tissue repair. If the injury is acute, then the normal tissue structure will be restored; however, continuous injury and inflammation dysregulates the normal healing process and leads to the accumulation of collagen, resulting in fibrosis [37]. Growth factors released during ECM degradation, cytokines secreted by HSCs or macrophages and the collagen accumulated during fibrogenesis work

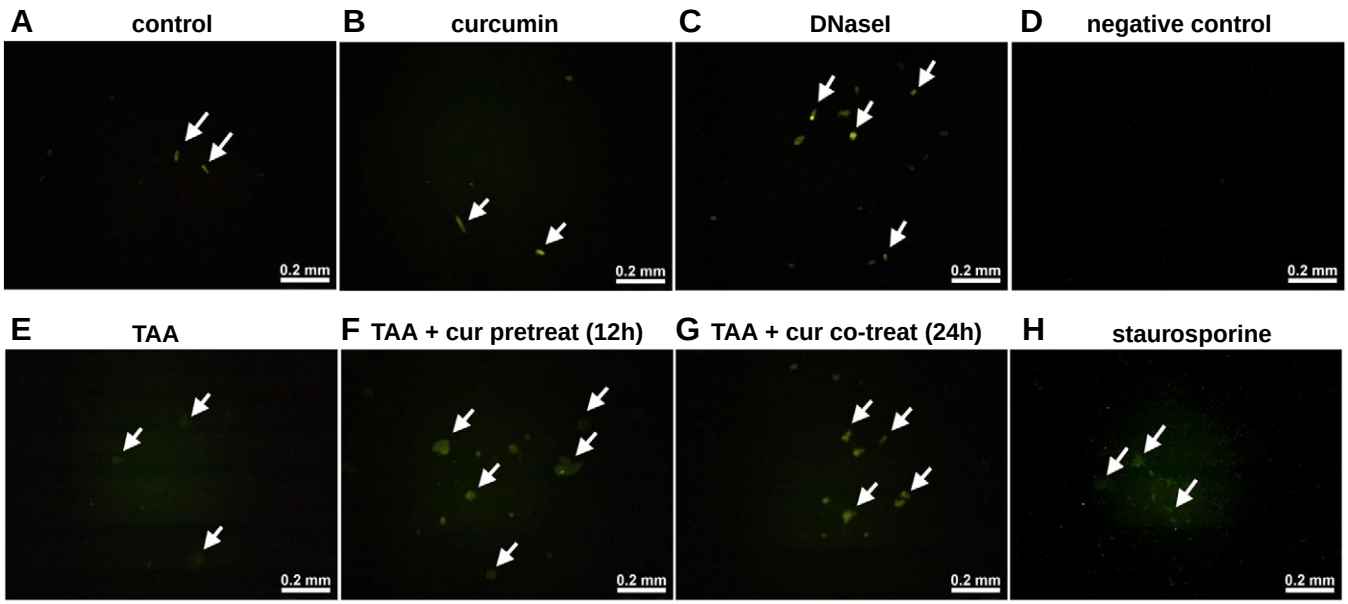

Fig. 12. TUNEL apoptosis assays on AML12 cells. TUNEL staining of cells with (A) mock treatment (negative control), (B) 24-h curcumin (20 μM) treatment, (C) 24-h DNase I (1500 U/ml) treatment (positive control), (D) no TdT added (negative control), (E) 24-h TAA (200 mM) treatment, (F) 12-h curcumin pretreatment followed by 12-h TAA treatment, (G) 24-h TAA+Cur cotreatment and (H) 24-h staurosporine (1 μM) treatment (apoptosis-positive control) are shown. White arrows indicate the apoptosis-positive cells with green fluorescent labeling.

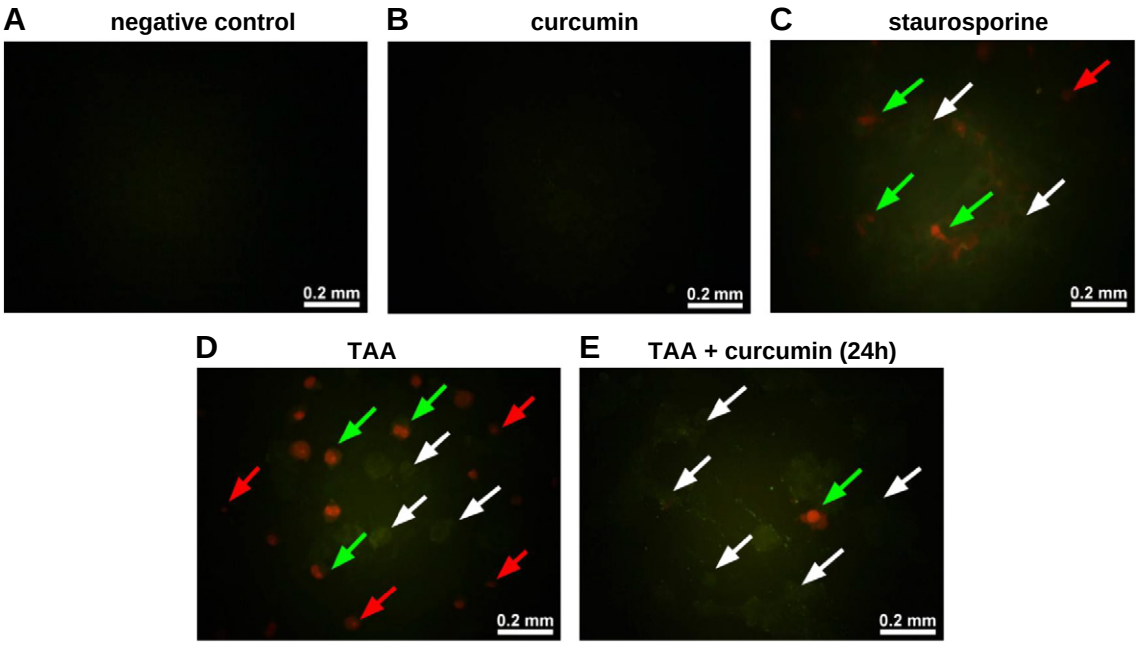

Fig. 13. Annexin V–FITC/PI apoptosis assays of AML12 cells. Cells were (A) left untreated (negative control) or treated with (B) curcumin (20 μM) for 24 h, (C) staurosporine (1 μM) (apoptosis-positive control), (D) TAA (200 mM) for 24 h or (E) TAA+Cur cotreatment for 24 h. Cells were then stained with annexin V–FITC and PI for 15 min in the dark and then observed by fluorescence microscopy. White arrows indicate apoptotic cells [annexin V-positive (green fluorescence)/PI-negative]. Red arrows indicate necrotic cells [PI-positive (red fluorescence)/annexin V-negative cells]. Green arrows indicate necrotic or late apoptotic cells [annexin V-positive/PI-positive cells].

together to stimulate cell proliferation [38]. Curcumin treatment induces damaged hepatocytes to undergo apoptosis by up-regulating P53 levels, as well as up-regulating proapoptotic and down-regulating antiapoptotic genes. Promotion of apoptosis not only decreases the number of necrotic cells during chronic liver injury, which inhibits the activation of inflammatory responses, but also prevents proliferation of hepatocytes containing damaged DNA that could progress to hepatocellular carcinoma. Together, we found that curcumin induces apoptosis of damaged hepatocytes and switches the liver damage response from progressive fibrogenesis to liver restoration. Thus, curcumin provides insight into potential therapies to prevent hepatic fibrosis after liver injury.

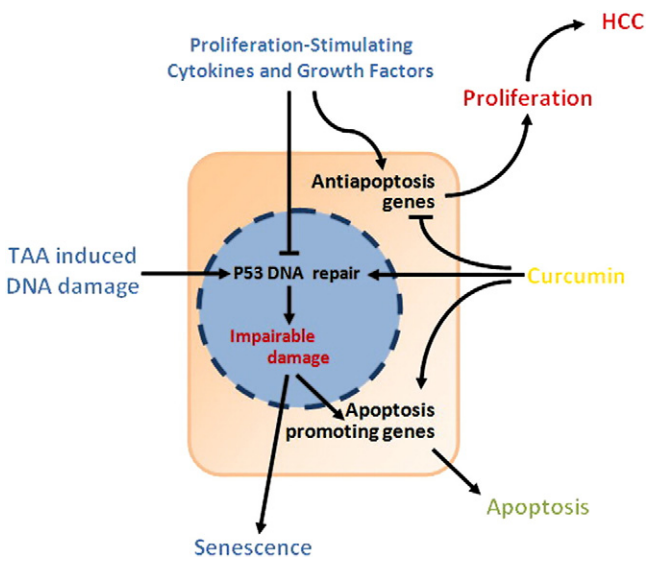

Fig. 14. Schematic model of the effect curcumin has on the expression of P53 and apoptosis-related genes that regulate the cell cycle after TAA-induced DNA damage of hepatocytes.

Acknowledgments

This research was supported by a grant from the National Science Council of Taiwan under contract NSC 98-2815-C-002-168-B.

References

[1] Friedman SL, Roll FJ, Boyles J, Bissell DM. Hepatic lipocytes: the principal collagen-producing cells of normal rat liver. Proc Natl Acad Sci U S A 1985;82:8681–5.
[2] Schultz GS, Wysocki A. Interactions between extracellular matrix and growth factors in wound healing. Wound Repair Regen 2009;17:153–62.
[3] Weber LW, Boll M, Stampfl A. Hepatotoxicity and mechanism of action of haloalkanes: carbon tetrachloride as a toxicological model. Crit Rev Toxicol 2003;33:105–36.
[4] Chilakapati J, Korrapati MC, Shankar K, Hill RA, Warbritton A, Latendresse JR, et al. Role of CYP2E1 and saturation kinetics in the bioactivation of thioacetamide: effects of diet restriction and phenobarbital. Toxicol Appl Pharmacol 2007;219:72–84.
[5] Kang JS, Wanibuchi H, Morimura K, Wongpoomchai R, Chusiri Y, Gonzalez FJ, et al. Role of CYP2E1 in thioacetamide-induced mouse hepatotoxicity. Toxicol Appl Pharmacol 2008;228:295–300.
[6] Hunter AL, Holscher MA, Neal RA. Thioacetamide-induced hepatic necrosis. I. Involvement of the mixed-function oxidase enzyme system. J Pharmacol Exp Ther 1977;200:439–48.
[7] Bataller R, Brenner DA. Liver fibrosis. J Clin Invest 2005;115:209–18.
[8] Barker EA, Smuckler EA. Nonhepatic thioacetamide injury. II. The morphologic features of proximal renal tubular injury. Am J Pathol 1974;74:575–90.
[9] Leclercq IA, Farrell GC, Sempoux C, dela Pena A, Horsmans Y. Curcumin inhibits NF-kappaB activation and reduces the severity of experimental steatohepatitis in mice. J Hepatol 2004;41:926–34.
[10] Reyes-Gordillo K, Segovia J, Shibayama M, Vergara P, Moreno MG, Muriel P. Curcumin protects against acute liver damage in the rat by inhibiting NF-kappaB, proinflammatory cytokines production and oxidative stress. Biochim Biophys Acta 2007;1770:989–96.
[11] Lin J, Chen A. Activation of peroxisome proliferator-activated receptor-gamma by curcumin blocks the signaling pathways for PDGF and EGF in hepatic stellate cells. Lab Invest 2008;88:529–40.
[12] Wu JC, Merlino G, Fausto N. Establishment and characterization of differentiated, nontransformed hepatocyte cell lines derived from mice transgenic for transforming growth factor alpha. Proc Natl Acad Sci U S A 1994;91:674–8.

[13] Mosmann T. Rapid colorimetric assay for cellular growth and survival: application to proliferation and cytotoxicity assays. J Immunol Methods 1983; 65:55–63.
[14] Bertrand R, Solary E, O'Connor P, Kohn KW, Pommier Y. Induction of a common pathway of apoptosis by staurosporine. Exp Cell Res 1994;211:314–21.
[15] Kuypers FA, Lewis RA, Hua M, Schott MA, Discher D, Ernst JD, et al. Detection of altered membrane phospholipid asymmetry in subpopulations of human red blood cells using fluorescently labeled annexin V. Blood 1996;87:1179–87.
[16] Kamiike W, Fujikawa M, Koseki M, Sumimura J, Miyata M, Kawashima Y, et al. Different patterns of leakage of cytosolic and mitochondrial enzymes. Clin Chim Acta 1989;185:265–70.
[17] Connolly KM, Bogdanffy MS. Evaluation of proliferating cell nuclear antigen (PCNA) as an endogenous marker of cell proliferation in rat liver: a dual-stain comparison with 5-bromo-2′-deoxyuridine. J Histochem Cytochem 1993;41:1–6.
[18] Brooks CL, Gu W. p53 ubiquitination: Mdm2 and beyond. Mol Cell 2006;21: 307–15.
[19] Meek DW. Tumour suppression by p53: a role for the DNA damage response? Nat Rev Cancer 2009;9:714–23.
[20] Schmitt CA, Fridman JS, Yang M, Baranov E, Hoffman RM, Lowe SW. Dissecting p53 tumor suppressor functions in vivo. Cancer Cell 2002;1:289–98.
[21] Tewari M, Quan LT, O'Rourke K, Desnoyers S, Zeng Z, Beidler DR, et al. Yama/CPP32 beta, a mammalian homolog of CED-3, is a CrmA-inhibitable protease that cleaves the death substrate poly(ADP-ribose) polymerase. Cell 1995;81:801–9.
[22] Darmon AJ, Nicholson DW, Bleackley RC. Activation of the apoptotic protease CPP32 by cytotoxic T-cell-derived granzyme B. Nature 1995;377:446–8.
[23] Taylor RC, Cullen SP, Martin SJ. Apoptosis: controlled demolition at the cellular level. Nat Rev Mol Cell Biol 2008;9:231–41.
[24] Martin SJ, Reutelingsperger CP, McGahon AJ, Rader JA, van Schie RC, LaFace DM, et al. Early redistribution of plasma membrane phosphatidylserine is a general feature of apoptosis regardless of the initiating stimulus: inhibition by overexpression of Bcl-2 and Abl. J Exp Med 1995;182:1545–56.
[25] Lin J, Zheng S, Chen A. Curcumin attenuates the effects of insulin on stimulating hepatic stellate cell activation by interrupting insulin signaling and attenuating oxidative stress. Lab Invest 2009;89:1397–409.
[26] Cao J, Liu Y, Jia L, Zhou HM, Kong Y, Yang G, et al. Curcumin induces apoptosis through mitochondrial hyperpolarization and mtDNA damage in human hepatoma G2 cells. Free Radic Biol Med 2007;43:968–75.
[27] Nakamura K, Yasunaga Y, Segawa T, Ko D, Moul JW, Srivastava S, et al. Curcumin down-regulates AR gene expression and activation in prostate cancer cell lines. Int J Oncol 2002;21:825–30.
[28] Shankar S, Chen Q, Sarva K, Siddiqui I, Srivastava RK. Curcumin enhances the apoptosis-inducing potential of TRAIL in prostate cancer cells: molecular mechanisms of apoptosis, migration and angiogenesis. J Mol Signal 2007;2:10.
[29] Chanvorachote P, Pongrakhananon V, Wannachaiyasit S, Luanpitpong S, Rojanasakul Y, Nimmannit U. Curcumin sensitizes lung cancer cells to cisplatin-induced apoptosis through superoxide anion-mediated Bcl-2 degradation. Cancer Invest 2009;27:624–35.
[30] Lin YL, Lin CY, Chi CW, Huang YT. Study on antifibrotic effects of curcumin in rat hepatic stellate cells. Phytother Res 2009;23:927–32.
[31] Diez-Fernandez C, Sanz N, Alvarez AM, Zaragoza A, Cascales M. Influence of aminoguanidine on parameters of liver injury and regeneration induced in rats by a necrogenic dose of thioacetamide. Br J Pharmacol 1998;125:102–8.
[32] Toledo F, Wahl GM. Regulating the p53 pathway: in vitro hypotheses, in vivo veritas. Nat Rev Cancer 2006;6:909–23.
[33] Vousden KH, Lane DP. p53 in health and disease. Nat Rev Mol Cell Biol 2007;8: 275–83.
[34] Lee DH, Rhee JG, Lee YJ. Reactive oxygen species up-regulate p53 and Puma; a possible mechanism for apoptosis during combined treatment with TRAIL and wogonin. Br J Pharmacol 2009;157:1189–202.
[35] Jaeschke H. Reactive oxygen and mechanisms of inflammatory liver injury: present concepts. J Gastroenterol Hepatol 2011;26(Suppl 1):173–9.
[36] Zhang M, Xu S, Han Y, Cao X. Apoptotic cells attenuate fulminant hepatitis by priming Kupffer cells to produce interleukin-10 through membrane-bound TGF-beta. Hepatology 2011;53:306–16.
[37] Bissell DM. Chronic liver injury, TGF-beta, and cancer. Exp Mol Med 2001;33: 179–90.
[38] Bissell DM, Choun MO. The role of extracellular matrix in normal liver. Scand J Gastroenterol Suppl 1988;151:1–7.